J. Biochem. **124**, 1051-1059 (1998)

Structures of Membrane Proteins Determined at Atomic Resolution[1]

Hiroaki Sakai and Tomitake Tsukihara[2]

Institute for Protein Research, Osaka University, 3-2 Yamada-oka, Suita, Osaka 565-0871

Received for publication, June 10, 1998

Following determination of the first crystal structure of the reaction center of *Rhodopseudomonas viridis*, a membrane protein, by X-ray crystal structure analysis at 3.0 Å resolution, 18 X-ray crystal structures and two electron crystal structures of membrane proteins have been obtained at higher than 3.5 Å resolution. Besides these integral membrane protein structures, three crystal structures of water-soluble proteins, which can enter membranes, have been determined by X-ray crystallography at high resolution. The structural features of membrane proteins have been summarized by inspecting these crystal structures. The polypeptide chain crosses the membrane in a helical conformation or a β-strand. The central +10 Å region of the transmembrane α-helix is dominated by hydrophobic residues. On both sides of the central region are concentrated polar aromatic residues. Charged residues are dominant around +15 Å to +20 Å. All the transmembrane β-structures are found in pore-forming proteins. The central region of the transmembrane β-structure is amphipathic with hydrophobic residues on the membrane exposed side. The distribution of amino acid residues on the membrane exposed surface of the transmembrane β-structure is similar to that of the transmembrane α-helix. α-Helices anchoring the membrane surface region are amphipathic with hydrophobic residues inside and hydrophilic residues outside.

Key words: membrane protein, X-ray crystal structure analysis.

Crystal structure analyses of integral membrane proteins

Proteins in the purple membrane of photosynthetic bacteria have been the most extensively studied among the various membrane proteins. Solar light energy is primarily absorbed by light-harvesting antenna complexes I (LH1) and II (LH2) and then transferred to the photosynthetic reaction center (RC). The RC uses the light energy with a very high quantum efficiency to transport electrons across the membrane. The crystal structure of the RC of *Rhodopseudomonas viridis* has revealed a new area in protein crystallography (*1*). Among the membrane proteins in solar light-energy conversion systems, the tertiary structures of RCs, LH2s, and a plant light-harvesting complex (LHC-II) have been determined at higher than 3.5 Å resolution, as listed in Table I. The projected structure of LH1 has been derived at 8.5 Å resolution by electron crystallography of the two-dimensional crystal (*9*). Plants and cyanobacteria contain photosystems I (PSI) and II (PSII) within the thylakoid membrane functioning during photosynthesis. The crystal structure of PSI at 4 Å resolution represents such structural model as 31 transmembrane helices and electron transfer pigments (*10*). However, we must await further structural analyses at higher resolution in order to inspect the structural features of this membrane protein.

Respiration is one of the typical energy conversion processes together with photosynthesis. The respiratory enzyme complexes, NADH dehydrogenase complex, cytochrome bc_1 complex and cytochrome *c* oxidase, are located in membranes and each of them acts as an electron-transport-driven proton pump. The X-ray structures of the cytochrome *c* oxidases from bovine heart (*14*) and *Paracoccus denitricans* (*17*) have both been determined at 2.8 Å resolution. Crystal structural analyses of respiratory membrane proteins are in progress, as shown in Table I.

Each biological membrane contains various channels that aid the selective transport of molecules or ions across it. Porins in the outer membranes of Gram-negative bacteria, mitochondria, and chloroplasts act as molecular sieves for hydrophilic molecules smaller than around 600 Da. Table I shows various channel proteins including porin whose tertiary structures have been determined at higher than 3.5 Å resolution. Colicins are antibiotic proteins that penetrate the outer membranes of sensitive *Escherichia coli* cells and kill them. The crystal structures of colicin Ia in a water-soluble state (*31*) and the water-soluble pore-forming domain of colicin A have been determined at 2.5 Å resolution (*32*).

Prostaglandin H2 synthase-1 is an integral membrane protein whose three-dimensional structure has been determined at 3.5 Å resolution (*33*). We review the structural features of such membrane proteins as photosynthetic protein complexes, respiratory complexes, pore-forming proteins, and a membrane-binding enzyme.

[1] The present work was partly supported by a grant from the "Research for the Future Program" of the Japan Society for the Promotion of Science. All protein figures were produced using the program, MOLSCRIPT (*42*). The atomic coordinates were taken from the Protein Data Bank (*43*).

[2] To whom correspondence should be addressed. Phone: +81-06-879-8605, Fax: +81-06-879-8606, E-mail: tsuki@protein.osaka-u.ac.jp

Structure of the anchor region of a monotopic membrane protein

Integral membrane proteins are classified as monotopic, bitopic, or polytopic according to the topology of the membranes spanned, as shown in Fig. 1 (*34*). Prostaglandin H2 synthase-1 is the only integral monotopic membrane protein whose crystal structure has been determined (*33*).

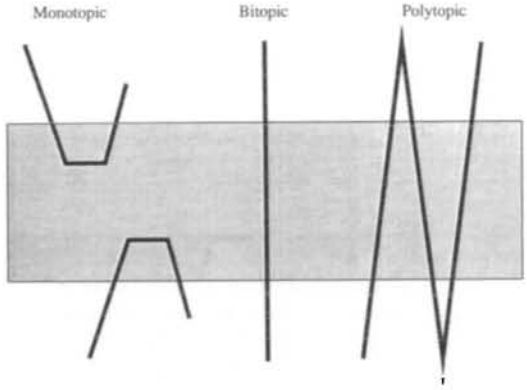

Fig. 1. **Classification of integral membrane proteins as monotopic, bitopic, or polytopic.** The hydrophobic region of the membrane is indicated by the gray belt.

Helices A, B, and C and the beginning of helix D are embedded in a shallow membrane region of the endoplasmic reticulum, as shown in Fig. 2a. These helices are roughly parallel to the membrane surface with the hydrophobic residues facing the inside of the membrane and rather hydrophilic residues being on the outer surface region of the membrane (Fig. 2, b, c, d, and e). The hydrophobic surfaces of these helices are formed by both aliphatic and aromatic hydrophobic groups which favorably interact with the hydrophobic tail groups of phospholipids. This interaction is analogous to the way in which surface-active peptides bind to the membranes (*35*). The opposite sides of the helices contain a few charged groups, which are well positioned to interact with the hydrophilic head groups of phospholipids. Since the amphipathic helices are not the most hydrophobic segments along the polypeptide chain, the membrane segments expected from the amino-acid sequence are incompatible with the crystal structure.

In any bitopic membrane protein whose crystal structure has been determined, the polypeptide chain crosses the membrane in a helical conformation

The a- and b-proteins of LH2, seven subunits of bovine heart cytochome *c* oxidase, one subunit of *P. denitricans* cytochrome *c* oxidase, four subunits of the cytochrome bc_1

TABLE I. **Structures of membrane proteins determined by X-ray and electron microscopy.**

Protein	Organism	Resolution (Å)	Method	Year	Reference
Proteins in light-energy conversion systems					
RC	*R. viridis*	3.0	X-ray	1984	*1, 2*
RC	*R. viridis*	2.3	X-ray	1995	*3*
RC	*R. sphaeroides*	2.8	X-ray	1987	*4*
RC	*R. sphaeroides*	2.65	X-ray	1994	*5*
LH2	*R. acidophila*	2.5	X-ray	1995	*6*
LH2	*R. molischianum*	2.4	X-ray	1996	*7*
LHC-II	Pea chloroplasts	3.4	EM	1994	*8*
Bacteriorhodopsin	*H. halobium*	3.5	EM	1996	*11*
Bacteriorhodopsin	*H. salinarium*	3.0	EM	1997	*12*
Bacteriorhodopsin	*H. salinarium*	2.5	X-ray	1996	*13*
Respiratory enzymes					
Complex IV (oxidized)	Bovine heart	2.8	X-ray	1995	*14, 15*
Complex IV (oxidized)	Bovine heart	2.3	X-ray	1998	*16*
Complex IV (reduced)	Bovine heart	2.35	X-ray	1998	*16*
Complex IV (CO-bound)	Bovine heart	2.8	X-ray	1998	*16*
Complex IV (N_3-bound)	Bovine heart	2.9	X-ray	1998	*16*
Complex IV (N_3-bound)	*P. denitricans*	2.8	X-ray	1995	*17*
Complex IV (oxidized)	*P. denitricans*	2.7	X-ray	1997	*18*
Complex III	Bovine heart	2.9	X-ray	1997	*19*
Complex III	Chicken	3.16	X-ray	1998	*20*
Complex III	Bovine heart	3.0	X-ray	1998	*21*
Channels					
Porin	*R. capsulatus*	1.8	X-ray	1991	*22-24*
OmpF	*E. coli*	2.4	X-ray	1992	*25*
PhoE	*E. coli*	3.0	X-ray	1992	*25*
LamB	*E. coli*	3.1	X-ray	1995	*26*
ScrY	*S. typhimurium*	2.4	X-ray	1998	*27*
Potassium channel	*S. lividans*	3.2	X-ray	1998	*28*
αHL pore	*S. aureus*	1.9	X-ray	1996	*29*
Aerolysin[a]	*A. hydrophila*	2.8	X-ray	1994	*30*

Abbreviations: RC, photosynthetic reaction center; LH2, light-harvesting antenna complex II; LHC-II, plant light-harvesting complex; Complex IV, cytochrome *c* oxidase; Complex III, cytochrome bc_1 complex; OmpF, matrix porin; PhoE, phosphoporin; LamB, maltoporin; ScrY, sucrose-specific porin; *R. viridis*, *Rhodopseudomonas viridis*; *R. sphaeroides*, *Rhodobacter sphaeroides*; *R. acidophila*, *Rhodopseudomonas acidophila*; *R. molischianum*, *Rhodospirillum molischianum*; *H. halobium*, *Halobacterium halobium*; *H. salinarium*, *Halobacterium salinarium*; *P. denitricans*, *Paracoccus denitricans*; *R. capsulatus*, *Rhodobacter capsulatus*; *E. coli*, *Escherichia coli*; *S. typhimurium*, *Salmonella typhimurium*; *S. lividans*, *Streptomyces lividans*; *S. aureus*, *Staphylococcus aureus*; *A. hydrophila*, *Aeromonas hydrophila*; EM, electron microscopy. [a]Monomeric aerolysin soluble in water.

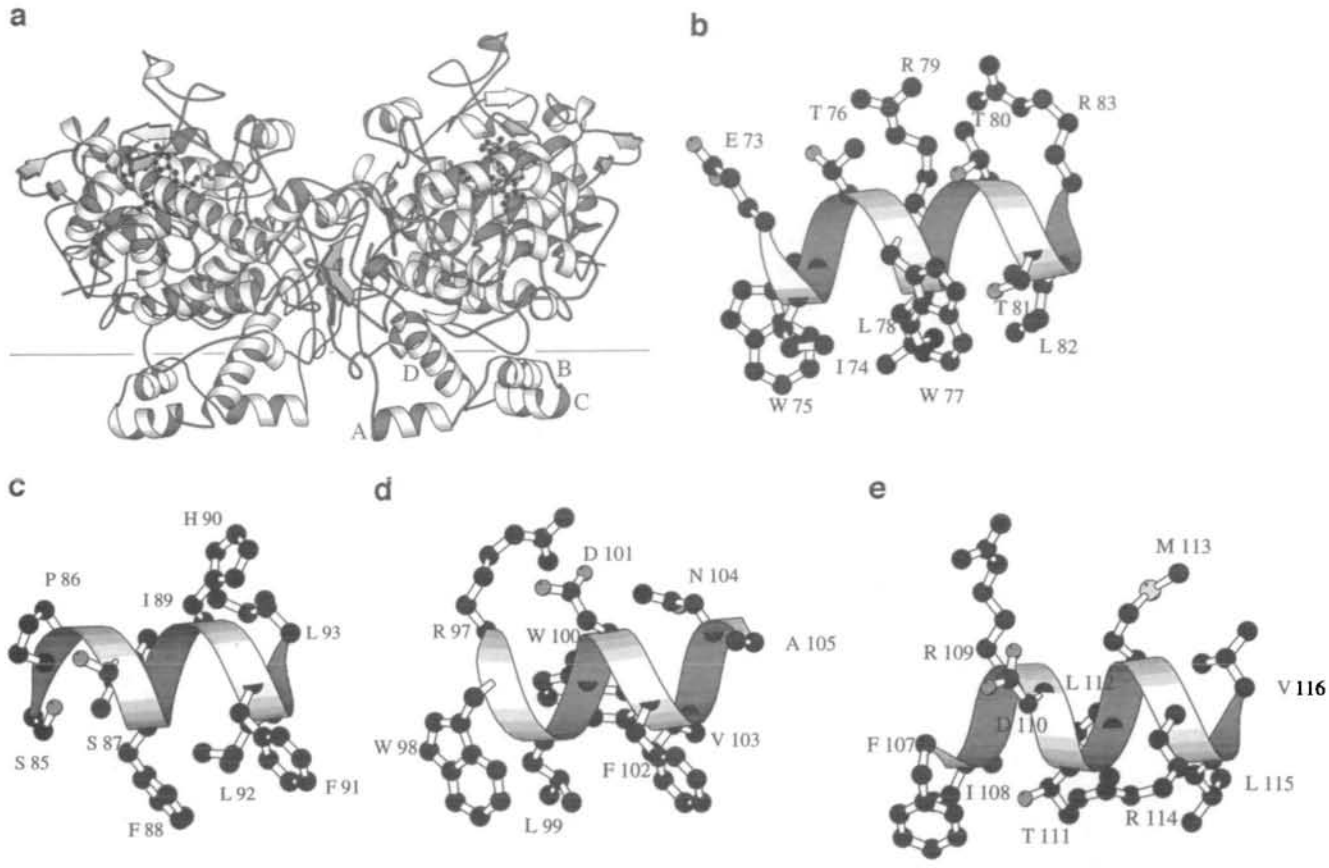

Fig. 2. (a) A ribbon drawing of the prostaglandin H2 synthase-1 dimer. The membrane surface is shown by the horizontal lines. The anchor helices denoted as A, B, C, and D are buried in the membrane. **(b) to (e) Schematic representations of helices A to D of the anchor region of prostaglandin H2 synthase-1.** Amino acid names are given by a single letter notation with a residue number. The upper and lower sides are the outer and inner surface of the membrane, respectively (PDB code 1PTH).

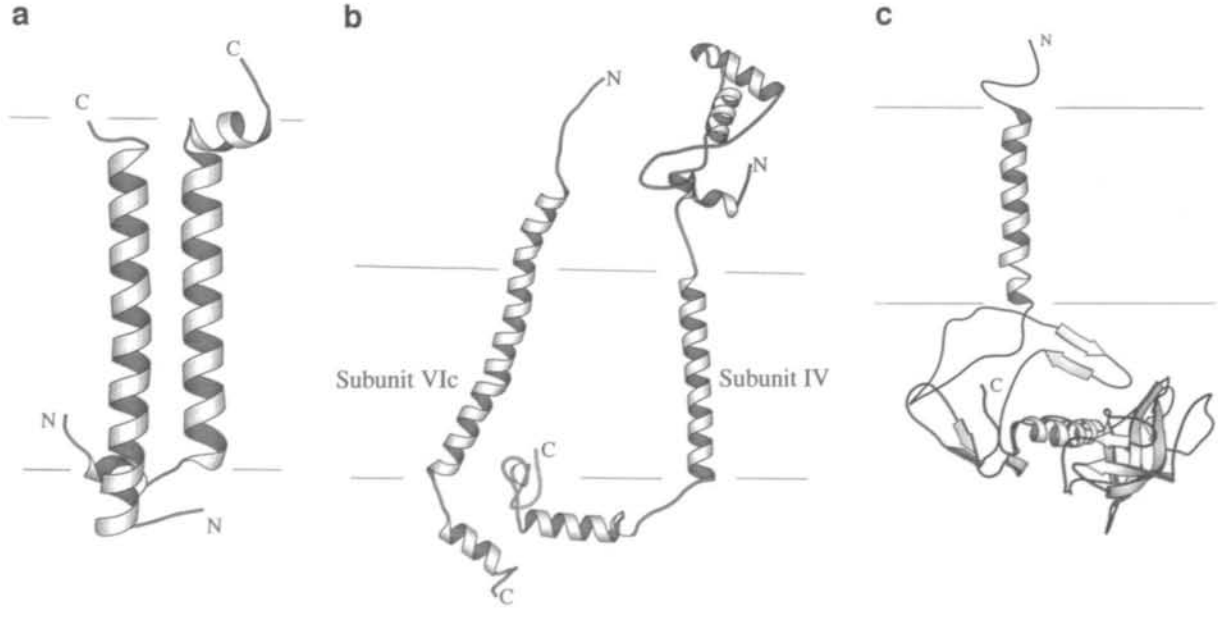

Fig. 3. Ribbon drawings of typical bitopic membrane proteins. Horizontal lines represent the membrane surfaces. N and C represent the amino and carboxyl termini, respectively. (a) Apoprotein a (left) and apoprotein b (right) of LH2 (PDB code 1KZU). (b) Nuclear subunits V and VII of bovine heart cytochrome *c* oxidase (PDB code 1OCC). (c) The H-subunit of the *R. viridis* RC (PDB code 1PRC).

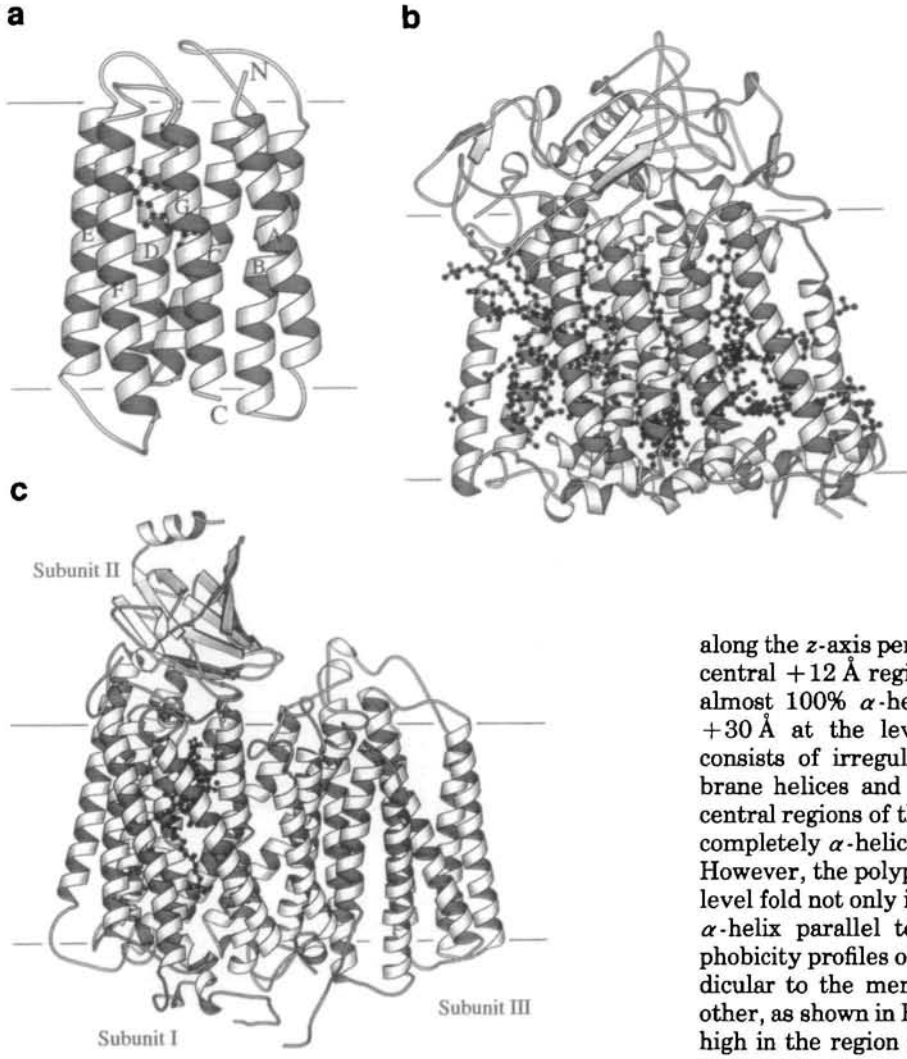

Fig. 4. **Ribbon drawings of polytopic membrane proteins, (a) bacteriorhodopsin (PDB code 2BRD), (b) the *R. sphaeroides* RC (PDB code 1PCR), and (c) the mitochondrial subunits of the bovine cytochrome *c* oxidase (PDB code 1OCC).** Cofactors are depicted by ball-and-stick models.

complex and the H-subunit of RC are all bitopic. The transmembrane segments of these proteins comprise helices with high hydrophobicities, as expected from their amino acid sequences. The transmembrane helices are nearly perpendicular to the membrane surface. Four typical bitopic membrane proteins are shown in Fig. 3, a, b, and c.

Both the amino-terminal and carboxyl-terminal regions of the a-protein of LH2 comprise amphipathic helices lying on both membrane surfaces like the A to D helices of prostaglandin H2 synthase 1. The first five residues of the b-protein of LH2 on the membrane surface have an extended conformation with alternating hydrophobic residues (Ala1, Leu3, and Ala5), and a short carboxyl-terminal tail lies on the membrane surface.

Bacteriorhodopsin, photosynthetic complexes, respiratory complexes, and a potassium channel are polytopic membrane proteins which cross the membrane in a helical conformation

Bacteriorhodopsin, the RC of *R. spheroides* and the mitochondrial subunits of bovine heart cytochrome *c* oxidase are typical helix bundle proteins, as shown in Fig. 4, a, b, and c. Wallin *et al.* (*36*) have analyzed the distribution of residues in the bovine cytochrome *c* oxidase along the *z*-axis perpendicular to the membrane plane. The central +12 Å region from the center of the membrane is almost 100% α-helix, whereas the region around +20–+30 Å at the level of the membrane surface mainly consists of irregular structures between the transmembrane helices and the globular peripheral domains. The central regions of the RC and bacteriorhodopsin are almost completely α-helices like that of the cytochrome *c* oxidase. However, the polypeptides of RC at the membrane surface level fold not only in irregular conformations but also in an α-helix parallel to the membrane surface. The hydrophobicity profiles of these proteins along the *z*-axis perpendicular to the membrane plane are very similar to each other, as shown in Fig. 5 (*36, 37*). The hydrophobicities are high in the region extending ~10 Å on either side of the center of the membrane, and then decrease to values typical for extramembrane parts in the next 10 Å. The mean hydrophobicity of the membrane-exposed residues of the 11 transmembrane helices is 0.36 and that of the buried interior residues is 0.22 (*38*). Membrane-exposed residues are also more hydrophobic than buried ones in the transmembrane region of the cytochrome *c* oxidase from bovine mitochondria (*36*). This hydrophobic organization is opposite to that of water-soluble proteins.

The distribution of charged residues and Trp residues of the RC from *R. viridis* is shown in Fig. 20b of the Ref. *39*. The central zone, where none of the charged residues is found, is about 25 Å thick. Amino acid distribution profiles of cytochrome *c* oxidase perpendicular to the membrane have been elucidated by Wallin *et al.* (*36*). The central +10 Å region is dominated by hydrophobic residues (Phe, Val, Leu, Met, and Ile). Around +12-15 Å there is a concentration of polar aromatic residues (Trp, Tyr) and amidated

[3] The hydrophobicity of a molecule is calculated from the relation: $\langle h \rangle = \Sigma c_i h_i$ where c_i is the molar fraction of the *i*th amino acid, h_i is the residue hydrophobicity, and the sum is over all 20 amino acids. The residue hydrophobicities are: Ala, 0.25; Arg, −1.76; Asn, −0.64; Asp, −0.72; Cys, 0.04; Glu, −0.62; Gln, −0.69; Gly, 0.16; His, −0.40; Ile, 0.73; Leu, 0.53; Lys, −1.10; Met, 0.26; Phe, 0.61; Pro, −0.07; Ser, −0.26; Thr, −0.18; Trp, 0.37; Tyr, 0.02; and Val, 0.54.

residues (Asn, Gln), closely followed by the appearance of charged residues (Asp, Glu, Arg, and Lys) around +15–20 Å.

Figure 6 shows the connections of the transmembrane helices of the L- and M-subunits of the RC to show the net charges at the ends of the helices and the helix connections. The cytoplasmic ends or connections are nearly always less negatively charged than the periplasmic side. Thus, the membrane proteins are strong electric dipoles. This asymmetric charge distribution correlates with the fact that the interior of bacteria is negatively charged, due to the action of electrogenic ion pumps. This means that the L- and M-subunits are oriented in the membrane in an energetically more favorable manner. This is called the "positive inside" rule by von Heijne (*40*). Asymmetry of the charge distribution between the two sides has also been found for mitochondrially encoded subunits of bovine cytochrome *c* oxidase (*41*). The matrix-facing parts of the mitochondrial subunits have higher contents of Arg and Lys residues than the parts facing the inter-membrane space. On the other hand, the bitopic membrane proteins of bovine cytochrome *c* oxidase encoded by nuclear DNAs do not obey the positive inside rule (*41*). This suggests that the structural organization of the bitopic membrane proteins is regulated by different factors from in the case of the mitochondrial subunits of the bovine cytochrome *c* oxidase.

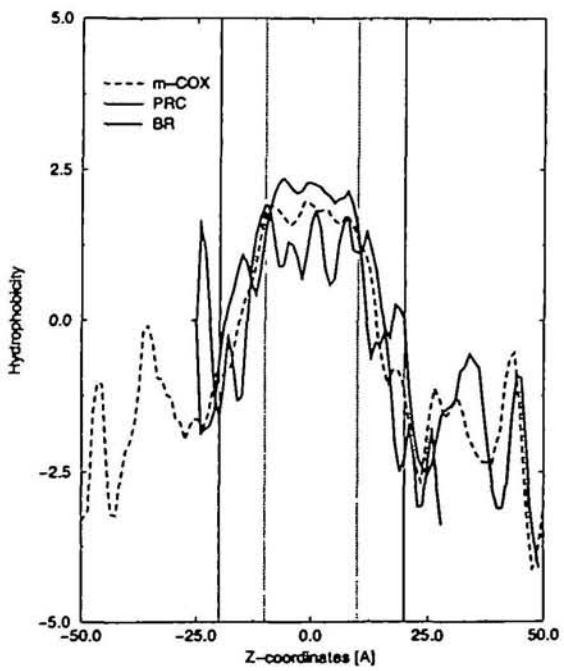

Fig. 5. **Average hydrophobicities of bovine cytochrome *c* oxidase (broken line), the *R. viridis* RC (continuous line), and bacteriorhodopsin (dotted line) in 5 Å slices.** The Z axis is perpendicular to the membrane surface [taken from Ref. *36* with permission: Wallin, E., Tsukihara, T., Yoshikawa, S., Von Heijne, G., and Elofsson, A. (1997) Architecture of helix bundle membrane proteins: An analysis of cytochrome *c* oxidase from bovine mitochondria. *Protein Sci.* **6**, 808–815; © 1997 Cambridge University Press].

Porins are polytopic membrane proteins consisting of an antiparallel β-barrel forming a pore which facilitates the diffusion of small molecules through membranes

The porin from *R. capsulatus* comprises a 16-stranded anti-parallel β-barrel crossing the membrane (*23*), as shown by the ribbon drawing in Fig. 7. OmpF and PhoE of *E. coli* have 16-stranded anti-parallel β-barrels similar to that of the porin from *R. capsulatus*, while LamB and SrcY have 18-stranded anti-parallel β-barrels. The β-barrels of the porins are different from the transmembrane α-helical bundles in the polarity of the transmembrane residues. The amino acid sequences of the porins are predominantly polar and do not have long hydrophobic segments like those found in transmembrane α-helical bundles. A hydrophobic band sandwiched between two tyrosine-belts separated by 25 Å has been identified on the membrane exposed surface of OmpF, as shown in Fig. 8 (*25*). The pore of PhoE is constricted to an elliptical cross-section of 7×11 Å by the internal loop structure from Arg100 to Ser134, as shown in Fig. 9. The pore has a lining of hydrophilic residues similar to the outer surface of water-soluble proteins. Other porins, such as that of *R. capsulatus*, OmpF and LamB, have aqueous pores like PhoE.

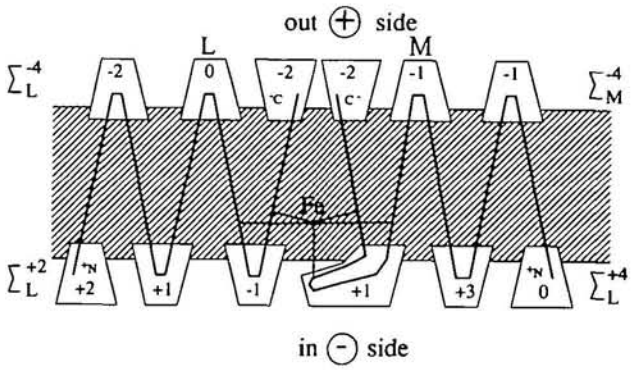

Fig. 6. **Schematic drawing of the transmembrane helices, and the helix connections of the L- and M-subunits of the *R. viridis* RC.** The cell interior and exterior are charged negatively and positively, respectively. The net charges at the end of helices and the helix connections are shown. The total net charge of the interior is +6 and that of the exterior is −8 (reproduced from Fig. 22 of Ref. *39*). © The Nobel Foundation 1989.

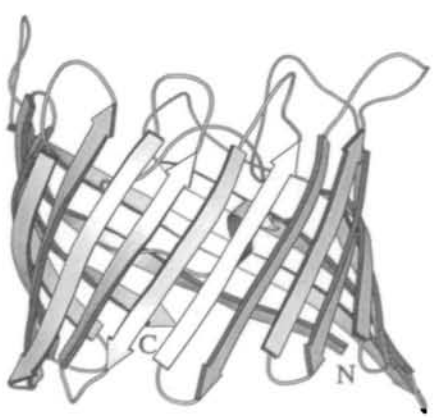

Fig. 7. **A ribbon drawing of the *R. capsulatus* porin (PDB code 1PRN).**

A potassium channel is formed by four identical subunits each consisting of three α-helices

The potassium channel of *S. lividans*, an integral membrane protein, is a tetramer with fourfold symmetry about a central pore. It has aromatic belts near the membrane surface level like other membrane proteins. Each subunit consists of a six-turn outer-helix, a three-turn pore helix, and an eight-turn inner helix. Four inner helices and four pore helices form a pore containing two potassium ions in the crystalline state (*28*).

αHL and aerolysin are transmembrane pores consisting of a β-barrel in the oligomeric state and are water-soluble proteins in the monomeric state

Figure 10, a and b, shows the monomeric and heptameric structures of αHL, respectively (*29*). The cap domain is composed of seven β sandwiches. Rim domains protrude from the underside of the heptamer. The stem domain consisting of a 14 stranded anti-parallel β-barrel forms a transmembrane channel. A crevice between the top of the stem domain and the rim domains defines a basic and aromatic amino acid-rich region that might interact with phospholipid head groups or other cell surface receptors (Fig. 10b). Through the stem, the diameter of the channel varies from 14 to 24 Å, depending on the size of the side chains protruding into the cylinder. Two hydrophobic bands, one formed by seven Met residues and the other by seven Leu residues, are solvent-exposed on the interior of the pore with sevenfold symmetry. Therefore, the interior of the pore is not as hydrophilic as that of the aqueous pores. A hydrophobic belt on the stem domain is defined by residues Tyr118, Phe120, Gly122, Val124, Gly126, Ile132, Gly134, Ile136, Ala138, Val140, and Ile142, and is about

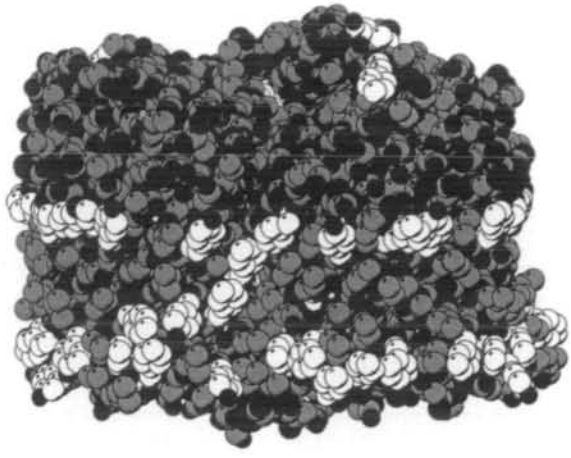

Fig. 8. **A space filling model of OmpF.** Oxygen and nitrogen atoms are in black, carbon atoms in gray, and the carbon atoms of aromatic side chains in white (PDB code 1OPF).

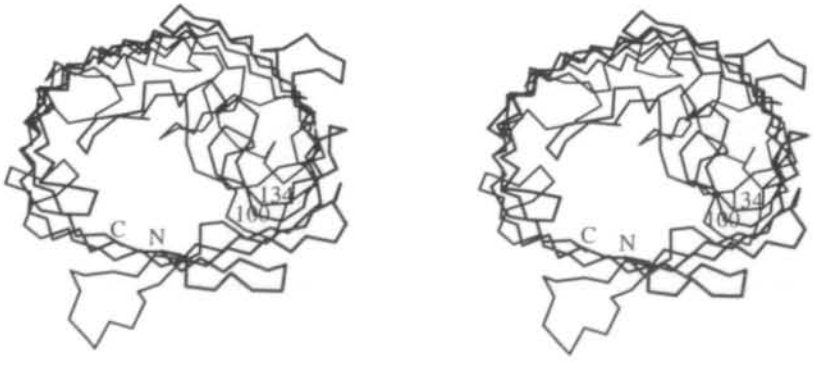

Fig. 9. **Stereoscopic Cα-drawing of PhoE shows a pore with an elliptical cross section of 7×11 Å.** The loop structure from Arg100 to Ser134 constricts the pore (PDB code 1PHO).

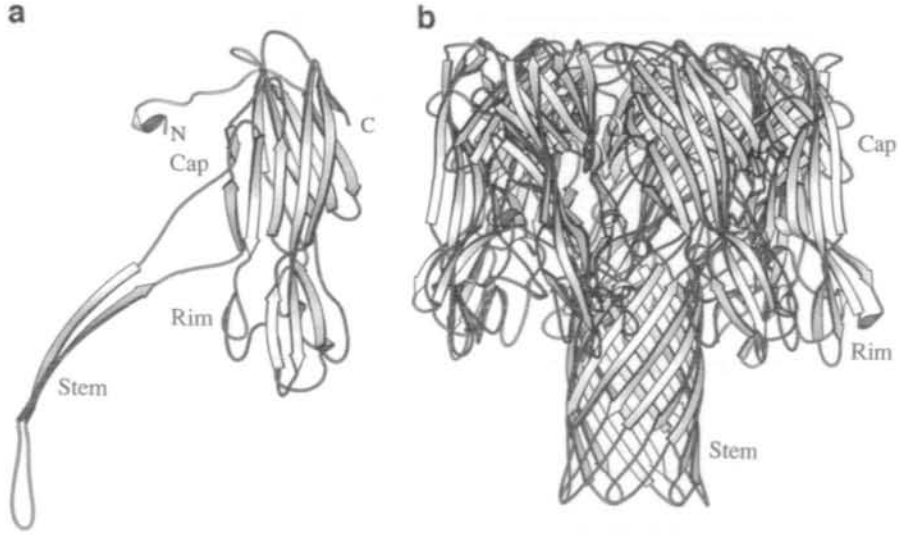

Fig. 10. **Ribbon drawings of (a) the αHL monomer and (b) the αHL heptamer (PDB code 7AHC).**

28 Å thick. A ring of 14 aromatic amino acids is composed of Tyr118 near the membrane surface and Phe120 on the inside of the membrane. Another mushroom-type structure (*30*) similar to that of αHL has been predicted for aerolysin from its monomeric structure determined by 2.8 Å X-ray analysis together with an image obtained by electron microscopy.

Colicin Ia has two 160-Å-long helices which enable the molecule to span the periplasmic space and simultaneously are in contact with both the outer and plasma membranes

Colicin Ia is about 210 Å long, and consists of three functional domains and a pair of 160-Å-long helices, as shown in Fig. 11 (*31*). An amino-terminal domain composed of α-helices seems to mediate the translocation across the outer membrane of the bacterial cells. The receptor binding domain consists of an amphipathic two-stranded β-hairpin and three α-helices. Although there is little sequence homology between the channel forming domains of colicin Ia and colicin A, they have the same arrangement of α-helices. Models for the membrane insertion and the channel formation of the channel forming domain of colicin A have been proposed (*32*). Out of ten

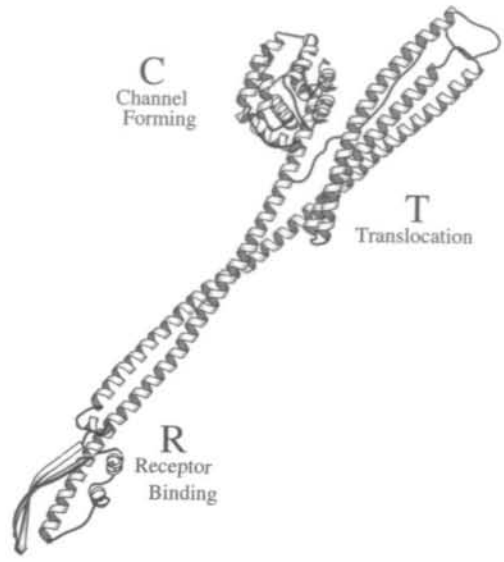

Fig. 11. **Ribbon drawing of the structure of colicin Ia consisting of channel-forming, translocation, and receptor-binding domains (PDB code 1ICC).**

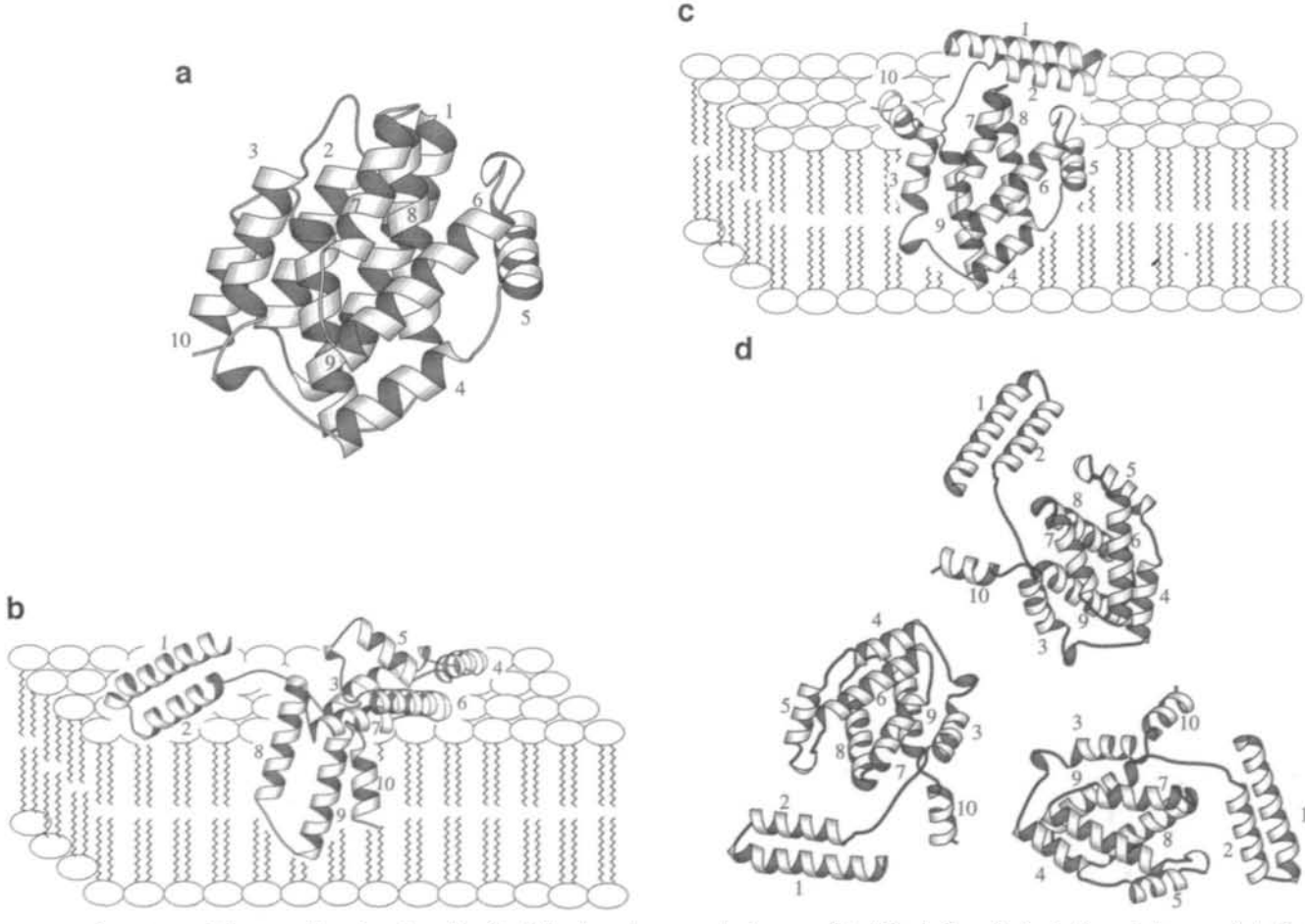

Fig. 12. **Structure of the pore-forming domain of colicin A and a proposed model for protein insertion into the membrane.** (a) Structure of the pore-forming domain. (b) The first step of insertion, the hydrophobic hairpins are inserted into the membrane. (c) The second step, amphipathic helices 3, 4, 5, 6, and 7 come into the membrane. (d) The third step, three proteins assemble to form a channel with a hydrophilic interior. A top view of the channel is shown (PDB code 1COL).

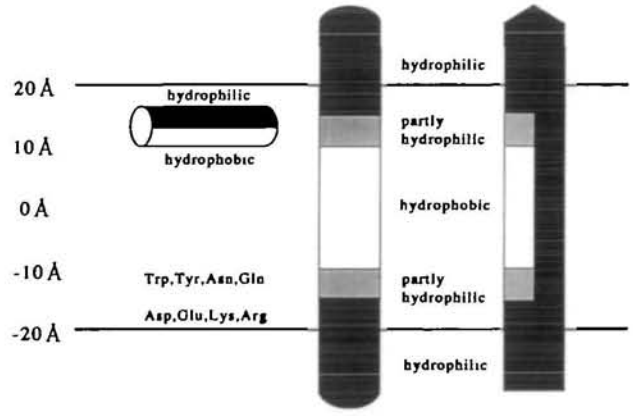

Fig. 13. **The structural features of membrane proteins are summarized.** The two horizontal lines at +20 Å show the membrane surfaces. White, gray, and black represent hydrophobic, partly hydrophilic, and hydrophilic regions. (Left) An amphipathic α-helix located near and parallel to the membrane surface, (middle) a transmembrane α-helix, and (right) a transmembrane β-structure are schematically drawn.

helices of the soluble state structure, two helices, 8 and 9, form a very hydrophobic hairpin. They are surrounded by eight amphipathic α-helices (Fig. 12a). In the first step of the membrane insertion, the hydrophobic hairpin of helices 8 and 9 comes into the membrane and the other eight amphipathic helices are located on the membrane surface with the hydrophobic part inside and the hydrophilic part outside (Fig. 12b). Application of a trans-negative membrane potential causes the insertion of helices 3, 4, 5, 6, and 7 (Fig. 12c), followed by trimerization to form the voltage-gated ion channel (Fig. 12d).

Concluding remarks

The general structural features of membrane proteins are summarized in Fig. 13. The polypeptide chain crosses the membrane in a helical conformation or a β-strand. Transmembrane α-helices have been found in bitopic membrane proteins and politopic α-helix bundles. The central +10 Å region is dominated by hydrophobic residues. On both sides of the central region there is a concentration of polar aromatic residues. Charged residues such as Asp, Glu, Arg, and Lys are dominant around +15 to +20 Å.

All the transmembrane β-structures have been found in pore-forming proteins. Each β-strand is amphipathic with the hydrophobic part exposed to the membrane and the hydrophilic part facing the interior of the pore. The distribution of individual residue types of the membrane-exposing part is similar to that of the transmembrane α-helix. The anchoring α-helix of a monotopic membrane protein is amphipathic, and is located parallel and close to the membrane surface. One side of the helix consisting of hydrophilic residues interacts with the polar head groups of phospholipids, and the other side with hydrophobic residues is in contact with the hydrophobic tails of the phospholipids.

REFERENCES

1. Deisenhofer, J., Epp, O., Miki, K., Huber, R., and Michel, H. (1984) X-Ray structure analysis of a membrane protein complex: electron density map at 3 Å resolution and a model of the chromatophores of the photosynthetic reaction center from *Rhodopseudomonas viridis*. *J. Mol. Biol.* **180**, 385-398
2. Deisenhofer, J., Epp, O., Miki, K., Huber, R., and Michel, H. (1985) Structure of the subunits in the photosynthetic reaction center of *Rhodopseudomonas viridis* at 3 Å resolution. *Nature* **318**, 618-624
3. Deisenhofer, J., Epp, O., Sinning, I., and Michel, H. (1995) Crystallographic refinement at 2.3 Å resolution and refined model of the photosynthetic reaction center from *Rhodopseudomonas viridis*. *J. Mol. Biol.* **246**, 429-457
4. Allen, J.P., Feher, G., Yeates, T., Komiya, H., and Rees, D.C. (1987) Structure of the reaction center from *Rhodobacter sphaeroides* R-26: The protein subunits. *Proc. Natl. Acad. Sci. USA* **84**, 6162-6166
5. Ermler, U., Fritzsch, G., Buchanan, S.K., and Michel, H. (1994) Structure of the photosynthetic reaction center from *Rhodobacter sphaeroides* at 2.65 Å resolution. *Structure* **2**, 925-936
6. McDermott, G., Prince, S.M., Freer, A.A., Hawthornthwaite-Lawless, A.M., Papiz, M.Z., Cogdell, R.J., and Isaacs, N.W. (1995) Crystal structure of an integral membrane light-harvesting complex from photosynthetic bacteria. *Nature* **374**, 517-521
7. Koepke, J., Hu, X., Muenke, C., Schulten, K., and Michel, H. (1996) The crystal structure of the light-harvesting complex II (B800-850) from *Rhodospirillum molischianum*. *Structure* **4**, 581-597
8. Kuhlbrandt, W., Wang, D.N., and Fujiyoshi, Y. (1994) Atomic model of plant light-harvesting complex by electron crystallography. *Nature* **367**, 614-621
9. Karrasch, S., Bullough, P., and Ghosh, R. (1995) The 8.5 Å projection map of the light-harvesting complex I from *Rhodospirillum rubrum* reveals a ring composed of 16 units. *EMBO J.* **14**, 631-638
10. Krauss, N., Schubert, W., Klukas, O., Fromme, P., Tobias, H., and Saenger, W. (1996) Photosystem I at 4 Å resolution represents the first structural model of a joint photosynthetic reaction centre and core antenna system. *Nat. Struct. Biol.* **3**, 965-973
11. Grigorieff, N., Ceska, T.A., Downing, K.H., Baldwin, J.M., and Henderson, R. (1996) Electron-crystallographic refinement of the structure of bacteriorhodopsin. *J. Mol. Biol.* **259**, 393-421
12. Kimura, Y., Vassylyev, D.G., Miyazawa, A., Kidera, A., Matsushima, M., Mitsuoka, K., Murata, K., Hirai, T., and Fujiyoshi, Y. (1997) Surface of bacteriorhodopsin revealed by high-resolution electron crystallography. *Nature* **389**, 206-211
13. Pebay-Peyroula, E., Rummel, G., Rosenbusch, J.P., and Landau, E.M. (1997) X-ray structure of bacteriorhodopsin at 2.5 angstroms from microcrystals grown in lipidic cubic phases. *Science* **277**, 1676-1681
14. Tsukihara, T., Aoyama, H., Yamashita, E., Tomizaki, T., Yamaguchi, H., Shinzawa-Itoh, K., Nakashima, R., Yaono, R., and Yoshikawa, S. (1995) Structure of metal sites of oxidized bovine heart cytochrome *c* oxidase at 2.8 Å. *Science* **269**, 1069-1074
15. Tsukihara, T., Aoyama, H., Yamashita, E., Tomizaki, T., Yamaguchi, H., Shinzawa-Itoh, K., Nakashima, R., Yaono, R., and Yoshikawa, S. (1996) The whole structure of the 13-subunit oxidized cytochrome *c* oxidase at 2.8 Å. *Science* **272**, 1136-1144
16. Yoshikawa, S., Shinzawa-Itoh, K., Nakashima, R., Yaono, R., Yamashita, E., Inoue, N., Yao, M., Fei, M.J., Peters Libeu, C., Mizushima, T., Yamaguchi, H., Tomizaki, T., and Tsukihara, T. (1998) Redox coupled structural changes in bovine heart cytochrome *c* oxidase at 2.3 Å resolution. *Science* **280**, 1723-1729
17. Iwata, S., Ostermeier, C., Ludwig, B., and Michel, H. (1995) Structure at 2.8 Å resolution of cytochrome *c* oxidase from *Paracoccus denitricans*. *Nature* **376**, 660-669
18. Ostermeier, C., Harrenga, A., Ermler, U., and Michel, H. (1997) Structure at 2.7 Å resolution of the *Paracoccus denitricans* two-subunit cytochrome *c* oxidase complexed with an antibody F_v fragment. *Proc. Natl. Acad. Sci. USA* **94**, 10547-10553
19. Xia, D., Yu, C., Kim, H., Xia, J., Kachurin, A.M., Zhang, L., Yu, L., and Deisenhofer, J. (1997) Crystal structure of the cyto-

chrome *bc*1 complex from bovine heart mitochondria. *Science* **277**, 60-66
20. Zhang, Z., Huang, L., Shulmeister, V.M., Chi, Y.-I., Kim, K.K., Hung, L.-W., Crofts, A.R., Berry, E.A., and Kim, S.-H. (1998) Electron transfer by domain movement in cytochrome *bc*1. *Nature* **392**, 677-684
21. Iwata, S., Lee, J.W., Okada, K., Lee, J.K., Iwata, M., Rasmussen, B., Link, T.A., Ramaswamy, S., and Jap, B.K. (1998) Complete structure of the 11-subunit bovine mitochondrial cytochrome *bc*1 complex. *Science* **281**, 64-71
22. Weiss, M.S., Kreusch, A., Schiltz, E., Nestel, U., Welte, W., Weckesser, J., and Schulz, G.E. (1991) The structure of porin from *Rhodobacter capsulatus* at 1.8 Å resolution. *FEBS Lett.* **280**, 379-382
23. Weiss, M.S., Abele, U., Weckesser, J., Welte, W., Schiltz, E., and Schulz, G.E. (1991) Molecular architecture and electrostatic properties of a bacterial porin. *Science* **254**, 1627-1630
24. Weiss, M.S. and Schulz, G.E. (1992) Structure of porin refined at 1.8 Å resolution. *J. Mol. Biol.* **227**, 493-509
25. Cowan, S.W., Schirmer, T., Rummel, G., Steiert, M., Ghosh, R., Pauptit, R.A., Jansonius, J.N., and Rosenbusch, J.P. (1992) Crystal structures explain functional properties of two *E. coli* porins. *Nature* **358**, 727-733
26. Schirmer, T., Keller, T.A., Wang, Y., and Rosenbusch, J.P. (1995) Structural basis for sugar translocation through maltoporin channels at 3.1 Å resolution. *Science* **267**, 512-514
27. Forst, D., Welte, W., Wacker, T., and Diederichs, K. (1998) Structure of the sucrose-specific porin ScrY from *Salmonella typhimurium* and its complex with sucrose. *Nat. Struct. Biol.* **5**, 37-46
28. Doyle, D.A., Cabral, J.M., Pfuetzner, R.A., Kuo, A., Gulbis, J.M., Cohen, S.L., Chait, B.T., and MacKinnon, R. (1998) The structure of the potassium channel: Molecular basis of K^+ conduction and selectivity. *Science* **280**, 69-77
29. Song, L., Hobaugh, M.R., Shustak, C., Cheley, S., Bayley, H., and Gouaux, J.E. (1996) Structure of staphylococcal α-hemolysin, a heptameric transmembrane pore. *Science* **274**, 1859-1866
30. Parker, M.W., Buckley, J.T., Postma, J.P.M., Tucker, A.D., Leonard, K., Pattus, F., and Tsernoglou, D. (1994) Structure of the aeromonas toxin proaerolysin in its water-soluble and membrane-channel states. *Nature* **367**, 292-295
31. Weiner, M., Freymann, D., Ghosh, P., and Stroud, R.M. (1997) Crystal structure of colicin Ia. *Nature* **385**, 461-464
32. Parker, M.W., Pattus, F., Tucker, A.D., and Tsernoglou, D. (1989) Structure of the membrane pore-forming fragment of cilocin A. *Nature* **337**, 93-96
33. Picot, D., Loll, P.J., and Garavito, R.M. (1994) The x-ray crystal structure of the membrane protein prostaglandin H2 synthase-1. *Nature* **367**, 243-249
34. Blobel, G. (1980) Intracellular protein topogenisis. *Proc. Natl. Acad. Sci. USA* **77**, 1496-1500
35. Kaiser, E.T. and Kezdy, F.A. (1987) Peptides with affinity for membranes. *Annu. Rev. Biophys. Chem.* **16**, 561-581
36. Wallin, E., Tsukihara, T., Yoshikawa, S., Von Heijne, G., and Elofsson, A. (1997) Architecture of helix bundle membrane proteins: An analysis of cytochrome *c* oxidase from bovine mitochondria. *Protein Sci.* **6**, 808-815
37. Eisenberg, D., Weiss, R.M., and Terwilliger, T.C. (1984) The hydrophobic moment detects periodicity in protein hydrophobicity. *Proc. Natl. Acad. Sci. USA* **81**, 140-144
38. Rees, D.C., DeAntonio, L., and Eisenberg, D. (1989) Hydrophobic organization of membrane proteins. *Science* **245**, 510-513
39. Deisenhofer, J. and Michel, H. (1989) The photosynthetic reaction center from the purple bacterium *Rhodopseudomonas viridis*. *Angew. Chem. Int. Ed. Engl.* **28**, 829-847
40. von Heijne, G. (1986) The distribution of positively charged residues in bacterial inner membrane proteins correlates with the trans-membrane topology. *EMBO J.* **5**, 3021-3027
41. Tomizaki, T., Yamashita, E., Yamaguchi, H., Aoyama, H., Tsukihara, T., Shinzawa-Itoh, K., Nakashima, R., Yaono, R., and Yoshikawa, S. (1998) Crystal structural analysis of bovine heart cytochrome *c* oxidase at 2.8 Å resolution. *Acta Cryst. D*, in press
42. Kraulis, P.J. (1991) MOLSCRIPT: A program to produce both detailed and schematic plots of protein structures. *J. Appl. Cryst.* **24**, 946-950
43. Bernstein, F.C., Koetzle, T.F., Williams, G.J., Meyer, E.F. Jr., Brice, M.D., Rodgers, J.R., Kennard, O., Shimanouchi, T., and Tasumi, M. (1977) The Protein Data Bank: A computer-based archival file for macromolecular structures. *J. Mol. Biol.* **112**, 535-542